

Flexible large area organic light emitting diode fabricated by electrohydrodynamics atomization technique

Memoon Sajid¹ · Muhammad Zubair^{1,4} · Yang Hoi Doh² · Kyoung-Hoan Na³ · Kyung Hyun Choi¹

Received: 10 March 2015 / Accepted: 7 June 2015 / Published online: 23 June 2015
© Springer Science+Business Media New York 2015

Abstract Large area organic light emitting diode (OLED) has been fabricated on flexible polyethylene terephthalate (PET) substrate using electrohydrodynamics spray system with active area of $3 \times 3 \text{ cm}^2$. This solution processing of organic inks and quantum dots is performed at room temperature and atmospheric pressure in a single step processing compatible with roll-to-roll processing system. The thin film characterizations are performed by SEM, TEM, spectroscopes and semiconductor device analyzer. CdSe/ZnS quantum dots are used as emissive layer while PEDOT:PSS and MEH-PPV are used as hole and electron transport layers. OLED produced red light at the wavelength of 634 nm. A life time of 1 h at 0.3 lx was achieved by the OLED device.

1 Introduction

Tang and Slyke [1] demonstrated the first organic light emitting diode (OLED) by using Alq₃ in 1987. From there on, a lot of research has been reported on OLEDs [2, 3]. The conjugated polymer devices have advantages like easy

fabrication, low cost, lightweight, human friendly, sustainable raw materials, very thin, large view angle, and fast response [4, 5]. The solution-based polymers make the fabrication process easier as compared to the inorganic conventional LEDs [6]. The LED lamps today achieve the most efficient lighting but OLEDs are even outperforming LEDs in performance [7]. Therefore, the future of lighting is flexible, thin, light, dimmable, low cost, solution processable and large area OLEDs. OLED lighting is highly efficient and has closest spectral distribution without any heat, UV emission, or glare [5, 8, 9].

Indium tin oxide (ITO) is generally used as the transparent bottom electrode of the device. ITO as anode provides holes to the device. Emissive layer is deposited between hole transport layers and electron transport layers. Top electrode is usually of reflective metal with low work function to provide electrons to the device [10–12].

Quantum dots are the nanocrystal with a quantum confinement [13, 14]. This quantum confinement enables them to narrow down the emission wavelengths that are tune able throughout the visible range [15]. The QDs have tunable band gap and are solution processable. These qualities makes them excellent candidates to be used in OLEDs [13, 16–18], solar cells [19–21], electroactive polymer artificial muscles [22], biological imaging [23–26] and composite materials. The quantum dots formed from heavy metals are used for imaging, diagnostics, and sensing purposes in medical science and are believed to be toxic. Ye et al. [27] show in a pilot study that rhesus macaques injected with phospholipid micelle encapsulated CdSe/CdS/ZnS quantum dots do not exhibit evidence of toxicity.

OLED thin films can be deposited by different printed electronics approaches like spin coating [4, 7, 11, 28, 29], transfer printing [30, 31], screen printing [32] and spray

✉ Kyung Hyun Choi
amm@jejunu.ac.kr

¹ Department of Mechatronics Engineering, Jeju National University, Jeju 690-756, South Korea

² Department of Electronic Engineering, Jeju National University, Jeju 690-756, South Korea

³ College of Engineering, Dankook University, Yongin-si, Gyeonggi-do, South Korea

⁴ Department of Electrical Engineering, College of Engineering, Majmaah University, Al-Majma'ah, Saudi Arabia

[33]. Here the focus is on large area OLED fabrication. Spin coating offers easy fabrication process but it is not suitable for large area applications. Spin coating has huge ink wastage, the process is not compatible with roll-to-roll system, masking is required and has low throughput [34]. In transfer printing, a thin films by spin coating or any other process is required before the material is transferred by using a stamp [35].

Electrohydrodynamics spray technique was used to fabricate the thin films. This technique is simple, easy, completed in a single step, and is performed in atmospheric temperature and pressure conditions. Various organic, inorganic inks have been sprayed by electrohydrodynamics spray in our previous work like poly(3,4-ethylenedioxythiophene):polystyrene sulfonate (PEDOT:PSS), zinc oxide (ZnO), zirconium dioxide (ZrO_2), carbon nanotubes, graphene flakes [28, 36–42].

In this work large area OLED is fabricated by using organic layers as hole and electron transport layers while quantum dots are used as emissive layer. Electrohydrodynamics spray process is used for the deposition of organic layers and quantum dots thin films with a device active area of $3 \times 3 \text{ cm}^2$. The poly[2-methoxy-5-(2-ethylhexyloxy)-1,4-phenylenevinylene] (MEH-PPV) ink has been optimized by adding ZnO nanoparticles for better spray. The thin layers and device are characterized for their surface, optical and electrical properties.

2 Experimental setup

2.1 Materials

The flexible polyethylene terephthalate (PET) substrate coated with indium tin oxide (ITO) was used with of surface resistivity $12 \Omega/\text{cm}^2$, MEH-PPV powder with average molecular weight around 40,000–70,000, cadmium oxide (CdO, 99.99 %), zinc acetate ($Zn(CH_3COO)_2$ 99.99 %, powder), oleic acid (OA, 90 %), trioctylphosphine (TOP, 90 %), selenium (Se, 99.99 %, powder), sulfur (S, 99.9 %, powder), 1-octadecene (90 %), dodecanethiol (99 %) and dimethyl sulfoxide (DMSO, 99.9 %) were purchased from Sigma Aldrich (South Korea). PEDOT:PSS was obtained from Agfa Materials Japan. Isopropanol and acetone were purchased from Deajon Chemicals and Metal Co, Ltd, South Korea. All chemical were used as received.

2.2 Inks preparation

The viscosity of PEDOT:PSS was reduced to 20 mPa s for better spray performance using isopropanol [43, 44]. The DMSO was added in ink for conductivity enhancement. The polymeric nature of PEDOT:PSS caused agglomerations

that were reduced by using Triton as a surfactant. The synthesis of CdSe/ZnS QDs is already reported in our previous work [33]. 5 wt% of quantum dots were dispersed in toluene while DMSO was used as co-solvent. The viscosity of quantum dots ink was 0.56 mPa s.

Different recipes for MEH-PPV electrohydrodynamics spray were used. In optimized recipe 0.2 % concentrated MEH-PPV solution was prepared from MEH-PPV powder by bath sonication with ice packs for 5 min and then magnetic stirring for 2 h. DMF was added to this solution in the ratio of 3:1. Solution was stirred for 30 min on magnetic stirrer. 0.05 % ZnO nanoparticles of average size of 40 nm were dispersed in the solution. The final viscosity of the solution was 6.2 mPa s. The ZnO nanoparticles were added to the ink solution to eliminate the electrospinning phenomena during electrohydrodynamics spray. The recipes for PEDOT:PSS, QDs and MEH-PPV inks are shown in Table 1.

2.3 Device fabrication

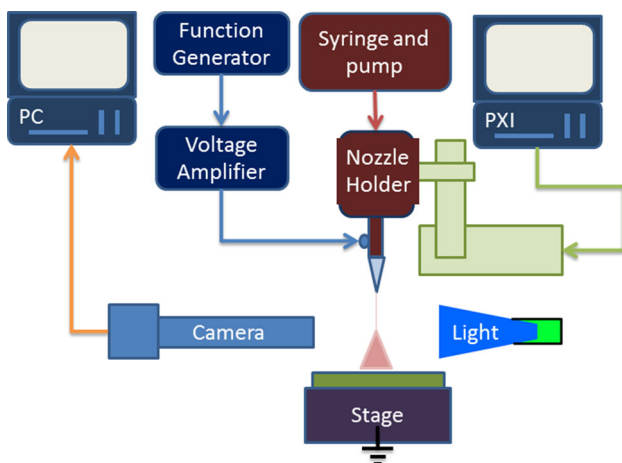
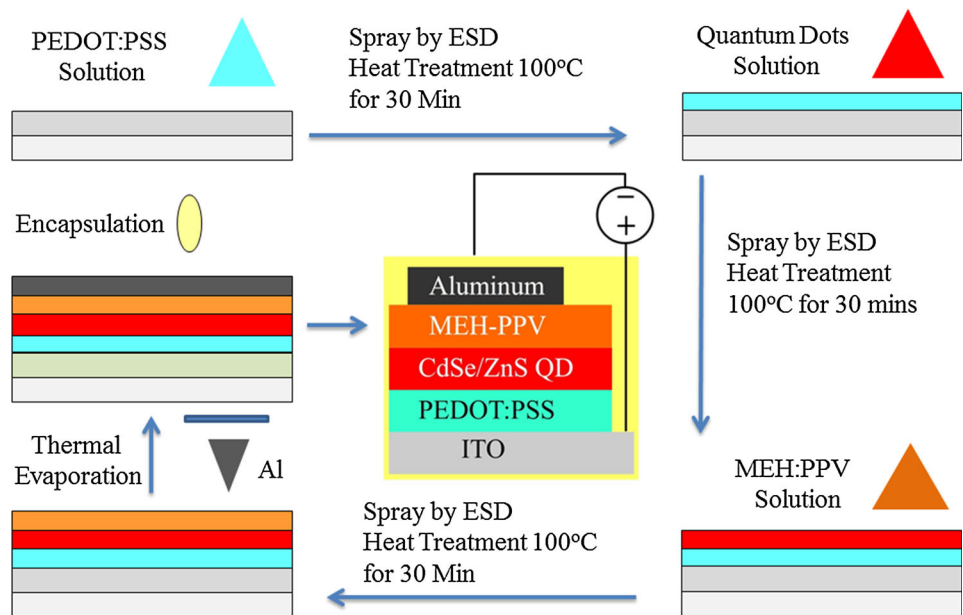
The device structure of fabricated OLED was ITO/PEDOT:PSS/(CdSe/ZnS QDs)/MEH-PPV/Al as shown in Fig. 1. The device was fabricated by electrohydrodynamics spray process. Initially ITO coated PET was cleaned by bath sonication using acetone and then isopropanol for 15 min each. After cleaning the ITO coated PET was rinsed with deionized water and dried by hot air. The organic contaminations present on substrate were removed by UV (ultraviolet) treatment for 120 s. The fabrication process is shown in Fig. 1. PEDOT:PSS was the first layer to be deposited on the ITO coated PET on an area of $4 \times 4 \text{ cm}^2$. The thin film was deposited by electrohydrodynamics spray process. The layer was dried at $100 \text{ }^\circ\text{C}$ for 30 min. CdSe/ZnS QDs were sprayed onto the dried PEDOT:PSS thin film by electrohydrodynamics spray system. The QDs thin film, used as emissive layer, was dried at $100 \text{ }^\circ\text{C}$ for an hour. MEH-PPV acted as electron transport layer. MEH-PPV was also sprayed by electrohydrodynamics spray. Thin film was dried after deposition at $100 \text{ }^\circ\text{C}$ for 30 min. The top electrode was deposited by thermal evaporation of aluminum. The deposition pressure was 10^{-6} torr with deposition rate of $3 \text{ \AA}/\text{s}$. The thickness of top electrode was 100 nm with active area of $3 \times 3 \text{ cm}^2$. Finally the device was encapsulated by a flexible epoxy binder.

2.4 Electrohydrodynamics spray setup

ESD setup is shown in Fig. 2. ESD was performed at room temperature and atmospheric pressure ($25 \text{ }^\circ\text{C}$, 50 % humidity). The in-house developed ESD system was fitted on a roll-to-roll system. The ESD system consists of a

Table 1 Recipe for PEDOT:PSS, quantum dots and MEH-PPV inks for EHDA spray

PEDOT:PSS	CdSe/ZnS QD	MEH-PPV
PEDOT:PSS: Isopropanol in 1:1.75 magnetic stirring for 4 h Ink + DMSO in 7:1 Magnetic stirring for 1 h Ink + Triton 40:1 Magnetic stirring for 1 h	5-wt% CdSe/ZnS dispersed in toluene with dimethyl sulfoxide (DMSO) as co-solvent	0.2 % of MEH-PPV in chloroform Bath sonication for 5 min with ice packs Magnetic stirring for 2 h Ink + DMF in 3:1 magnetic stirring for 1 h Ink + ZnO in 1:0.05 Magnetic stirring for 1 h

Fig. 1 OLED step by step fabrication process and the structure of device**Fig. 2** Electrohydrodynamics spray deposition (ESD) system setup

metallic capillary, nozzles with different internal diameters such as 110, 210 and 310 μm were selected on the bases ink parameters like viscosity, molecular weights of organic inks, particle size of inorganic materials and standoff distances. A

nozzle adaptor (NanoNC) was connected to a syringe (Hamilton, Model 1001 GASTIGHT syringe). This syringe was connected to an infusion pump (Harvard Apparatus, PHD 2000 Infusion) by Teflon tubing. The infusion pump controlled the flow rate of inks. The nozzle adaptor was attached to a head holder that can move in x, y and z axis using linear servomotors. LabVIEW (version 8.6) was used to control the motion of head holder using a motion controller card (NI PXI 7340) installed in PXI (NI-PXI-8110). To interface the linear servomotor with motion controller card, an interface board (CW7764YS3) was used. A program was written in LabVIEW to move the head holder in prescribed path by coordinates mentioned in a text file. The metallic nozzle was connected to high voltage supply (TREK Model 610E) while the base was connected to ground on which substrate was placed. The voltage signal was generated by a function generator (Hewlett Packard 33120A). The electrohydrodynamics phenomena was observed by a high speed camera (Motion Pro X) laminated by a light source (Moritex MLET-A080W1LRD).

2.5 Characterization

Thin films surface morphology was analyzed by field emission scanning electron microscopy (FE-SEM Model JEOL JSM-7600F, Japan). The FE-SEM was operated at accelerating voltage of 5 kV. The size and lattice spacing of quantum dots was observed by high resolution transmission electron microscope (HRTEM Model JEOL JEM 2100F). Thickness of thin films was measured by reflectometer (K-MAC ST4000-DLX). The optical analysis of thin films on ITO coated PET were done by using a ultraviolet/visible spectrometer (Shimadzu UV-3150) in range of 300–800 nm UV–visible (UV–Vis) data. Photoluminance of thin films was performed by photoluminance spectroscopy (Parkin Elmer LS-55) with 365 nm excitation wavelength. The electrical analysis of devices was performed by Agilent B1500A Semiconductor Device Analyzer coupled with MST8000C Probe Station having a current resolution of 1 fA. The HOMO and LUMO values of the QDs were determined from the cyclic voltammetry (CV) for which a three electrode electrochemical cell was used with a potentiostat (VSP, Bio-Logic). We used a glassy carbon disk as a working electrode, a Pt wire as a counter electrode, and a Ag/0.01 M AgNO₃ + 0.1 M tetrabutylammonium hexafluorophosphate (TBAPF₆) acetonitrile (Ag/Ag+) as a reference electrode. The CV measurements were done from –2.0 to 1.7 V at a scan rate of 20 mV/s. The electroluminescence spectra of the films were measured by an Avantes AVA-SPEC 2048 calibrated spectrometer. Minolta LS-100 luminance meter was used to measure luminous intensity and to collect the Commission International d’Eclairage (CIE) coordinators (x,y) for the identification of color.

3 Results and discussion

3.1 Electrohydrodynamics spray

Electrohydrodynamics atomization process is used to spray the functional inks onto the substrate under the effect of electric field. Without any electric field, functional ink flowing through the nozzle results in drops larger than the external diameter of nozzle. The phenomenon is known as dripping mode of electrohydrodynamics. As the electric field is applied and increased gradually, the drop size starts to decrease. This mode of atomization is known as the microdripping mode. With further increase in voltage, a cone is observed at the meniscus in an unstable form. Increase in voltage takes the unstable cone jet to a stable jet. Further increase in voltage results in multijet.

MEH-PPV was used as electron transport layer. The conductivity of this polymer was increased by DMF for

better spray performance. According to the classical electrohydrodynamic atomization of the stable cone jet mode, the electrical relaxation time, T_e , must be very much smaller than the hydrodynamic time, T_h . It is established by the inequality [45].

$$\frac{\beta \epsilon_0}{K} \ll \frac{LD}{Q} \tag{1}$$

where β is the relative permittivity, K is the electrical conductivity, L is the axial length of the jet, D is the jet diameter, Q is the given flow rate and ϵ_0 is the permittivity of vacuum (8.85×10^{-12} F/m). Here DMSO increases the conductivity of ink, which results in reduction of the electrical relaxation time. The lower relaxation time results in satisfying the inequality and achieve better spray results. ZnO nanoparticles were added in small quantity to remove electrospinning phenomena. Electrospinning for even a very small duration throughout spray process would result in porous thin film. The different recipes used for the electrospray are shown in Table 2. The spray of the different functional inks was performed in stable cone jet mode. The parameters for the spray of PEDOT:PSS, CdSe/ZnS QDs and MEH-PPV are presented in Table 3.

3.2 Surface morphology

The surface morphology of organic thin films was analyzed by FE-SEM. Figure 3 shows the FE-SEM images of PEDOT:PSS and MEH-PPV. The FE-SEM images showed no signs of pores or defects on the thin films. The CdSe/ZnS QDs were analyzed by HR-TEM as shown in Fig. 4. The quantum dots showed average particle size of 8 nm. The lattice spacing was found out to be 0.4 nm. The thickness of thin films of PEDOT:PSS, QDs and MEH-PPV were 100, 105 and 120 nm respectively.

3.3 Optical analysis

The photoluminescence of QDs showed a peak at wavelength of 634 nm as shown in Fig. 5. The electroluminescence of the OLED device also showed a wavelength around 634 nm. The electroluminescence produced by OLED

Table 2 MEH-PPV ink recipes for electrohydrodynamics spray

Inks ratio	Sprayability		Electrospinning	
MEH-PPV	DMF	ZnO NPs		
3 (0.5 %)	1	No	No	Yes
1 (0.5 %)	1	No	No	Yes
1 (0.5 %)	3	No	No	Yes
3 (0.3 %)	1	No	Yes	Yes
3 (0.2 %)	1	1:0.05	Yes	No

Table 3 Parameters of electrohydrodynamics spray of PEDOT:PSS, CdSe/ZnS QD and MEH-PPV

Parameter	PEDOT:PSS	CdSe/ZnS QDs	MEH-PPV
Nozzle internal diameter (μm)	310	110	210
Flow rate ($\mu\text{l/h}$)	750	270	1000
Viscosity of ink (mPa s)	20	0.56	6.2
Standoff distance (mm)	10	6	15
Voltage (kV)	4.3	2.8	6.01
Speed (mm/s)	3	3	3
Number of passes	8	4	4
Spray area (cm^2)	4.5×4.5	4.5×4.5	4.5×4.5
Drying time (min)	30	60	30
Drying temperature ($^{\circ}\text{C}$)	100	100	100

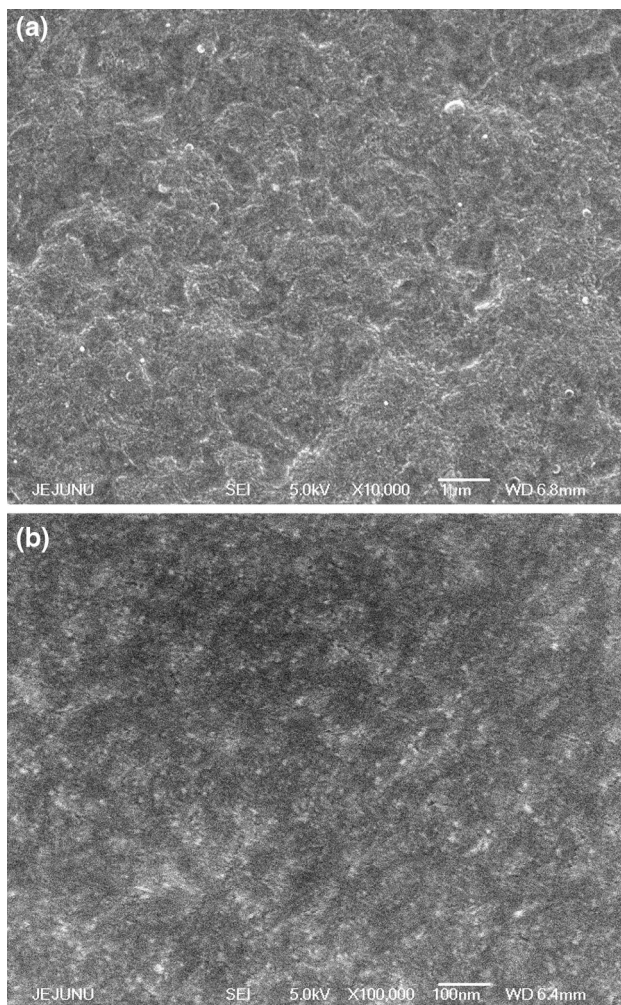


Fig. 3 SEM images of **a** PEDOT:PSS layer and **b** MEH:PPV layer

showed that QD acted as the emissive layer and MEH-PPV acted as electron transport layer. This electroluminescence at 634 nm wavelength lies in red color region. The electroluminescence is shown in Fig. 6.

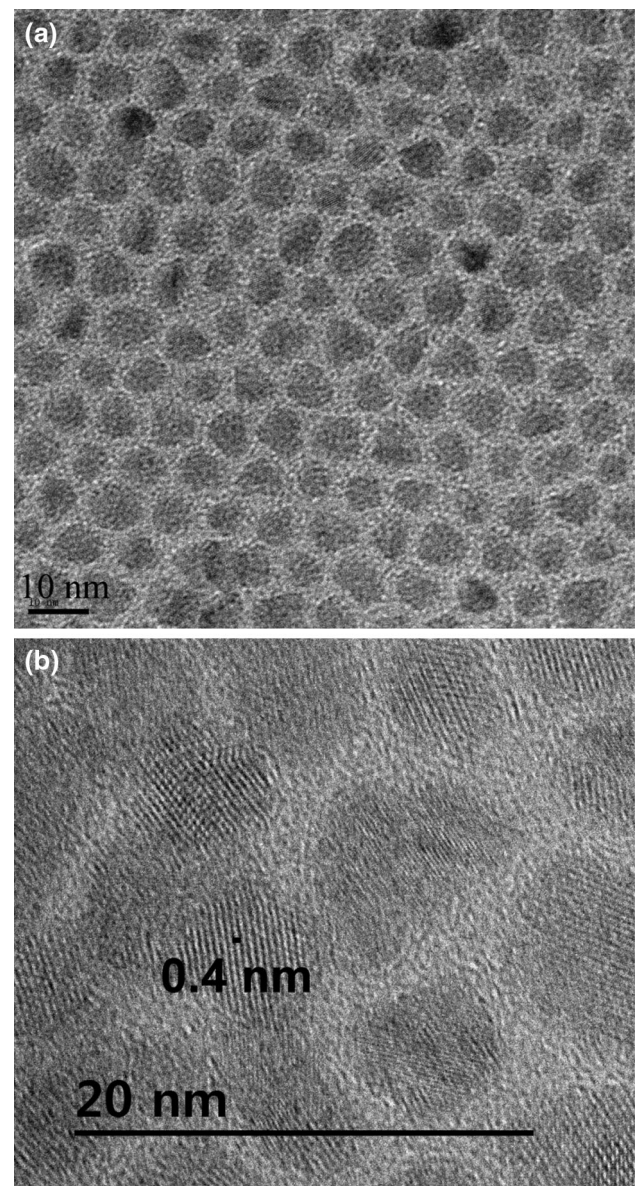


Fig. 4 TEM images of the CdSe quantum dots showing their size

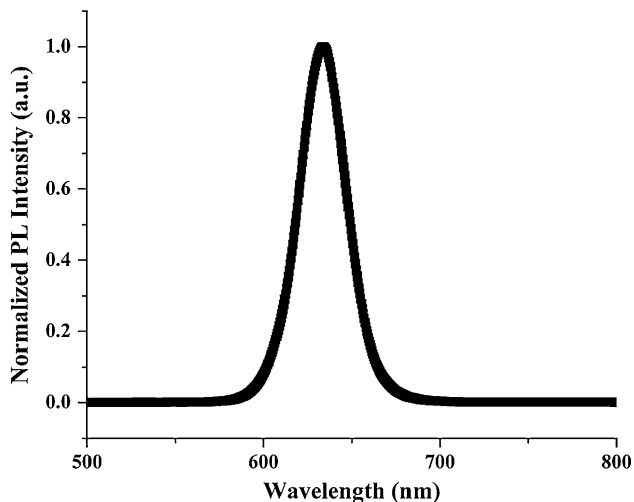


Fig. 5 Photo luminescence curve of the quantum dots

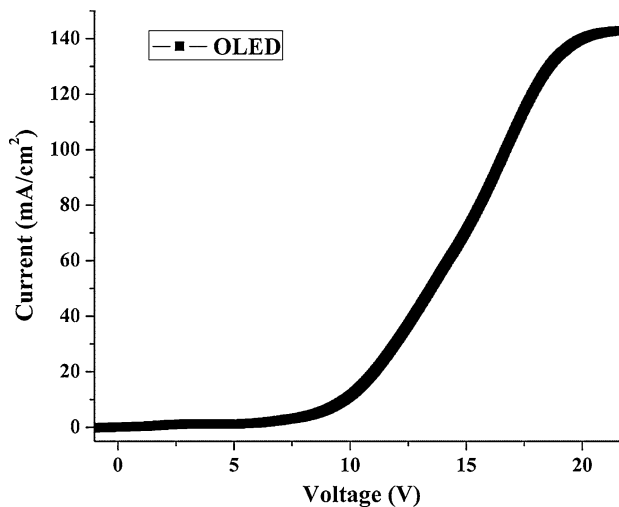


Fig. 7 I–V characteristic curve of the organic light emitting diode

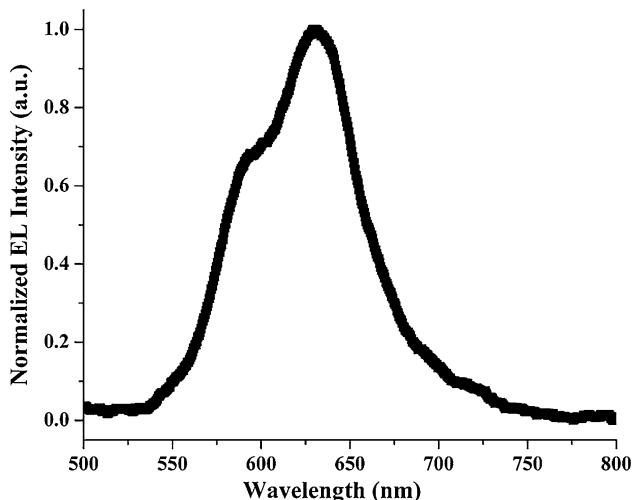


Fig. 6 Electro luminescence curve of the fabricated OLED

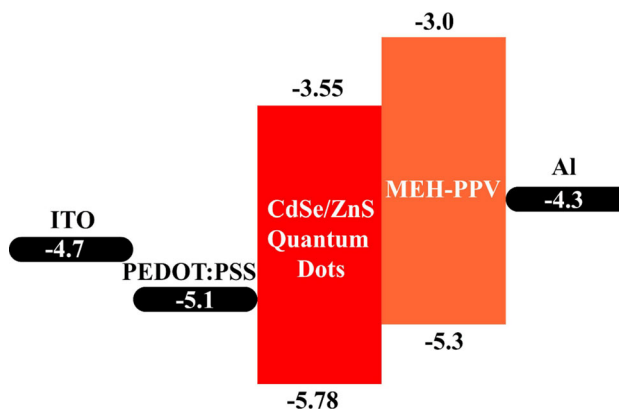


Fig. 8 Layer by layer energy band diagram of the device

3.4 Electrical characterization

The electrical analysis of OLED was performed as shown in the Fig. 7. I–V shows the turn on voltage of 5 V and maximum current density of 143 mA/cm². Here it can be seen that device (ITO/PEDOT:PSS/QDs/MEH-PPV/Al) shows non-ideal, schottky diode behavior with hopping charge transport mechanism [15, 46]. The energy level of QDs was measured and HOMO/LUMO values of QDs were -5.785 and -3.55 eV. The energy level diagram of the device is shown in Fig. 8. The luminance of the OLED was measured by lux meter and maximum 0.5 lx was obtained as shown in Fig. 9. The luminance of OLED was uniform and without any defects. The lifetime of fabricated devices was measured to be more than an hour. The Commission International d’Eclairage (CIE) coordinates

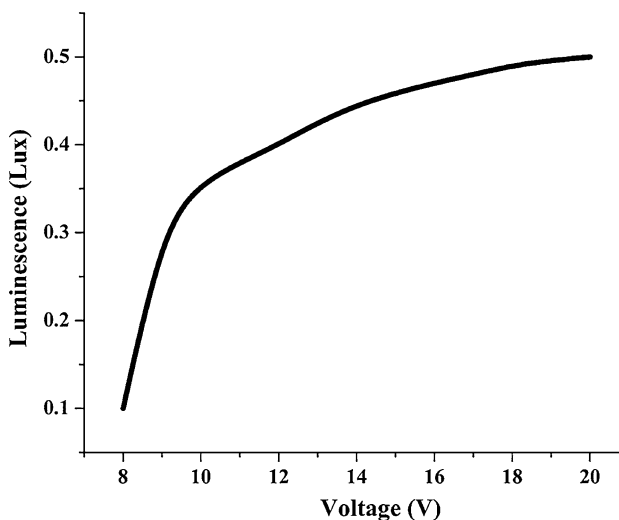


Fig. 9 Luminescence versus voltage curve of the OLED

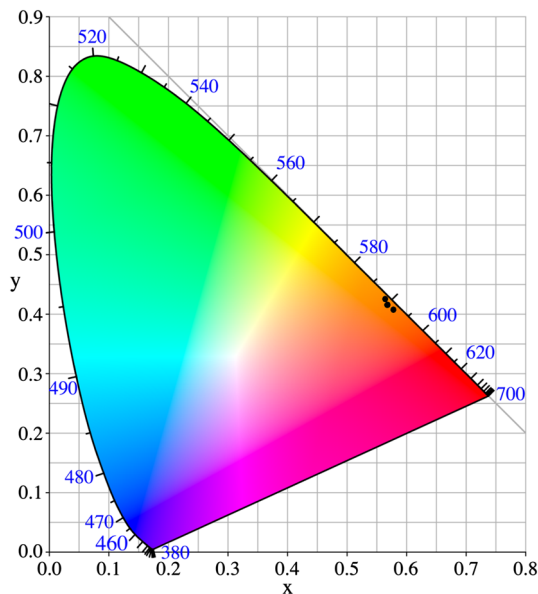


Fig. 10 Commission International d'Eclairage (CIE) coordinates for the OLED

were obtained by the lux meter which were (0.6, 0.39) which is in red color range as shown in Fig. 10. This large area, flexible, solution based, roll-to-roll processed OLED offers the answer to the high demands of lighting applications in near future.

4 Conclusions

The large area OLED fabricated by ESD process with an active area of OLED is $3 \times 3 \text{ cm}^2$ has been fabricated and characterized. CdSe/ZnS QDs are used as the emissive layer with emission wavelength of 634 nm lying in red color region. The conjugate polymers of PEDOT:PSS and MEH-PPV have been used as hole and electron transport layers to facilitate the movement of charge carriers from electrodes to emissive layer. The average size of QDs was 8 nm with lattice spacing of 0.4 nm. The spray of MEH-PPV has been optimized by adding nanoparticles of ZnO. The OLED device has shown the current density of 143 mA/cm^2 at 20 V. Maximum luminance of 0.5 lx has been achieved with CIE color coordinates (0.6, 0.39). The encapsulated device remained active for more than an hour. Thus, the simple structure device with optimized charge transport and emissive layers fabricated by spray system installed on roll-to-roll system offer a good potential for future lighting applications.

Acknowledgments This work was supported by the National Research Foundation of Korea (NRF) Grant funded by the Korea government (MSIP) (No. NRF-2014R1A2A1A01007699).

Conflict of interest The authors declare no conflict of interest.

References

1. C.W. Tang, S.a. VanSlyke, Organic electroluminescent diodes. *Appl. Phys. Lett.* **51**, 913 (1987). doi:10.1063/1.98799
2. D.I. Son, B.W. Kwon, D.H. Park, W.-S. Seo, Y. Yi, B. Angadi et al., Emissive ZnO-graphene quantum dots for white-light-emitting diodes. *Nat. Nanotechnol.* **7**, 465–471 (2012). doi:10.1038/nnano.2012.71
3. C.X. Guo, Y. Dong, H. Bin Yang, C.M. Li, Graphene quantum dots as a green sensitizer to functionalize ZnO nanowire arrays on F-doped SnO_2 glass for enhanced photoelectrochemical water splitting. *Adv. Energy Mater.* **3**, 997–1003 (2013). doi:10.1002/aenm.201300171
4. M. Mustafa, M. Zubair, H.C. Kim, K.H. Choi, Fabrication and characterization of organic light emitting diodes by using solution processable conjugated polymer. *J. Nanoelectron. Optoelectron.* **8**, 343–348 (2013). doi:10.1166/jno.2013.1478
5. S.R. Forrest, The road to high efficiency organic light emitting devices. *Org. Electron.* **4**, 45–48 (2003). doi:10.1016/j.orgel.2003.08.014
6. H.T. Nguyen, N.D. Nguyen, S. Lee, Application of solution-processed metal oxide layers as charge transport layers for CdSe/ZnS quantum-dot LEDs. *Nanotechnology* **24**, 115201 (2013). doi:10.1088/0957-4484/24/11/115201
7. A.P. Kulkarni, C.J. Tonzola, A. Babel, S.a. Jenekhe, Electron transport materials for organic light-emitting diodes. *Chem. Mater.* **16**, 4556–4573 (2004). doi:10.1021/cm0494731
8. Y. Leterrier, C. Fischer, L. Médico, F. Demarco, J.E. Månson, P. Bouten, et al., Mechanical properties of transparent functional thin films for flexible displays, in *46th Annual Technical Conference Proceedings*, vol. 3 (Society of Vacuum Coaters 505/856-7188, 2003), pp. 3–8
9. N. Thejo Kalyani, S.J. Dhoble, Organic light emitting diodes: energy saving lighting technology—a review. *Renew. Sustain. Energy Rev.* **16**, 2696–2723 (2012). doi:10.1016/j.rser.2012.02.021
10. F. Wang, H. Li, P. Chang, The real anode and the electrons-pump-layer of OLED. *Optoelectron. Adv. Mat.* **5**, 610–612 (2011)
11. M.M. de Kok, M. Buechel, S.I.E. Vulto, P. van de Weijer, E.a. Meulenkaamp, S.H.P.M. de Winter et al., Modification of PEDOT:PSS as hole injection layer in polymer LEDs. *Phys. Status Solidi* **201**, 1342–1359 (2004). doi:10.1002/pssa.200404338
12. D. Credginton, *Nano-scale Lithography and Microscopy of Organic Semiconductors* (PhD Thesis, University College London, 2010)
13. D. Bera, L. Qian, T.-K. Tseng, P.H. Holloway, Quantum dots and their multimodal applications: a review. *Materials* **3**, 2260–2345 (2010). doi:10.3390/ma3042260
14. V. Wood, V. Bulović, Colloidal quantum dot light-emitting devices. *Nano Rev.* **1**, 1–7 (2010). doi:10.3402/nano.v1i0.5202
15. A.J. Houtepen, Charge injection and transport in quantum confined and disordered systems, Utrecht University, 2007
16. L. Zhao, Z. Zhou, Z. Guo, J. Pei, S. Mao, Development of New Polymer Systems and Quantum Dots—Polymer Nanocomposites for Flexible OLED Display Applications (2011)
17. S. He, S. Li, F. Wang, A.Y. Wang, J. Lin, Z. Tan, Efficient quantum dot light-emitting diodes with solution-processable molybdenum oxide as the anode buffer layer. *Nanotechnology* **24**, 175201 (2013). doi:10.1088/0957-4484/24/17/175201
18. V. Gupta, N. Chaudhary, R. Srivastava, G.D. Sharma, R. Bhardwaj, S. Chand, Luminescent graphene quantum dots for organic photovoltaic devices. *J. Am. Chem. Soc.* **133**(26), 9960–9963 (2011). doi:10.1021/ja2036749

19. A.K. Rath, M. Bernechea, L. Martinez, G. Konstantatos, Solution-processed heterojunction solar cells based on p-type PbS quantum dots and n-type Bi₂S₃ nanocrystals. *Adv. Mater.* **23**, 3712–3717 (2011). doi:[10.1002/adma.201101399](https://doi.org/10.1002/adma.201101399)
20. Sa McDonald, G. Konstantatos, S. Zhang, P.W. Cyr, E.J.D. Klem, L. Levina et al., Solution-processed PbS quantum dot infrared photodetectors and photovoltaics. *Nat. Mater.* **4**, 138–142 (2005). doi:[10.1038/nmat1299](https://doi.org/10.1038/nmat1299)
21. T. Fukuda, K. Takagi, T. Asano, Z. Honda, N. Kamata, K. Ueno et al., Bulk heterojunction organic photovoltaic cell fabricated by the electrospray deposition method using mixed organic solvent. *Phys. Status Solidi-Rapid Res. Lett.* **5**, 229–231 (2011). doi:[10.1002/pssr.201105232](https://doi.org/10.1002/pssr.201105232)
22. M.H.J. Oh, M. Chen, C.-H. Chuang, G.J. Wilson, C. Burda, M.a Winnik et al., Charge transfer in CdSe nanocrystal complexes with an electroactive polymer. *J. Phys. Chem. C* **117**, 18870–18884 (2013). doi:[10.1021/jp406196a](https://doi.org/10.1021/jp406196a)
23. Y. Wang, L. Chen, Quantum dots, lighting up the research and development of nanomedicine. *Nanomedicine* **7**, 385–402 (2011). doi:[10.1016/j.nano.2010.12.006](https://doi.org/10.1016/j.nano.2010.12.006)
24. M. Han, X. Gao, J.Z. Su, S. Nie, Quantum-dot-tagged microbeads for multiplexed optical coding of biomolecules. *Nat. Biotechnol.* **19**, 631–635 (2001). doi:[10.1038/90228](https://doi.org/10.1038/90228)
25. T. Jamieson, R. Bakhshi, D. Petrova, R. Pocock, M. Imani, A.M. Seifalian, Biological applications of quantum dots. *Biomaterials* **28**, 4717–4732 (2007). doi:[10.1016/j.biomaterials.2007.07.014](https://doi.org/10.1016/j.biomaterials.2007.07.014)
26. J.K. Jaiswal, H. Mattoussi, J.M. Mauro, S.M. Simon, Long-term multiple color imaging of live cells using quantum dot bioconjugates. *Nat. Biotechnol.* **21**, 47–51 (2003). doi:[10.1038/nbt767](https://doi.org/10.1038/nbt767)
27. L. Ye, K.-T. Yong, L. Liu, I. Roy, R. Hu, J. Zhu et al., A pilot study in non-human primates shows no adverse response to intravenous injection of quantum dots. *Nat. Nanotechnol.* **7**, 453–458 (2012). doi:[10.1038/nnano.2012.74](https://doi.org/10.1038/nnano.2012.74)
28. M. Mustafa, H.C. Kim, Y. Doh, K.H. Choi, Structural, optical, and electrical characterization of (2, 1, 3)-thiadiazole thin film fabricated by electrostatic spray technique. *Polym. Eng. Sci.* (2013). doi:[10.1002/pen](https://doi.org/10.1002/pen)
29. B. Kang, D. Kim, S. Yeom, K. Kim, J. Seo, J. Kim, et al., Fabrication of organic/inorganic LED device using nanocrystal quantum dots as active layer, in *2010 IEEE 5th International Conference on Nano/Micro Engineered and Molecular Systems* (2010), pp. 832–835. doi:[10.1109/NEMS.2010.5592227](https://doi.org/10.1109/NEMS.2010.5592227)
30. T. Kim, K. Cho, E.K. Lee, S.J. Lee, J. Chae, J.W. Kim et al., Full-colour quantum dot displays fabricated by transfer printing. *Nat. Photonics* (2011). doi:[10.1038/NPHOTON.2011.12](https://doi.org/10.1038/NPHOTON.2011.12)
31. B.S. Mashford, M. Stevenson, Z. Popovic, C. Hamilton, Z. Zhou, C. Breen et al., High-efficiency quantum-dot light-emitting devices with enhanced charge injection. *Nat. Photonics* **7**, 407–412 (2013). doi:[10.1038/nphoton.2013.70](https://doi.org/10.1038/nphoton.2013.70)
32. D.a. Pardo, G.E. Jabbour, N. Peyghambarian, Application of screen printing in the fabrication of organic light-emitting devices. *Adv. Mater.* **12**, 1249–1252 (2000). doi:[10.1002/1521-4095\(200009\)12:17<1249:AID-ADMA1249>3.0.CO;2-Y](https://doi.org/10.1002/1521-4095(200009)12:17<1249:AID-ADMA1249>3.0.CO;2-Y)
33. M. Zubair, M. Mustafa, K. Lee, C. Yoon, Y.H. Doh, K.H. Choi, Fabrication of CdSe/ZnS quantum dots thin film by electrohydrodynamics atomization technique for solution based flexible hybrid OLED application. *Chem. Eng. J.* **253**, 325–331 (2014). doi:[10.1016/j.cej.2014.05.067](https://doi.org/10.1016/j.cej.2014.05.067)
34. H. Lee, A. Kim, S.M. Cho, H. Chae, Characterization of thermal annealing of gravure printed PVK/Ir(ppy)₃ organic light emitting layers. *Curr. Appl. Phys.* **10**, e143–e146 (2010). doi:[10.1016/j.cap.2010.08.029](https://doi.org/10.1016/j.cap.2010.08.029)
35. J. Lim, W.K. Bae, J. Kwak, S. Lee, C. Lee, K. Char, Perspective on synthesis, device structures, and printing processes for quantum dot displays. *Opt. Mater. Express.* **2**, 594 (2012). doi:[10.1364/OME.2.000594](https://doi.org/10.1364/OME.2.000594)
36. N. Duraisamy, N.M. Muhammad, M.-T. Hyun, K.-H. Choi, Structural and electrical properties of P3HT:PCBM/PEDOT:PSS thin films deposited through electrohydrodynamic atomization technique. *Mater. Lett.* **92**, 227–230 (2013). doi:[10.1016/j.matlet.2012.10.104](https://doi.org/10.1016/j.matlet.2012.10.104)
37. N. Duraisamy, N. Malik, A. Ali, J. Jo, K. Choi, Film deposited through electrohydrodynamic atomization technique. *Mater. Lett.* **83**, 80–83 (2012). doi:[10.1016/j.matlet.2012.05.127](https://doi.org/10.1016/j.matlet.2012.05.127)
38. N. Duraisamy, S.-J. Hong, K.-H. Choi, Deposition and characterization of silver nanowires embedded PEDOT:PSS thin films via electrohydrodynamic atomization. *Chem. Eng. J.* **225**, 887–894 (2013). doi:[10.1016/j.cej.2013.04.007](https://doi.org/10.1016/j.cej.2013.04.007)
39. N.M. Muhammad, N. Duraisamy, H.-W. Dang, J. Jo, K.-H. Choi, Solution processed Al doped ZnO film fabrication through electrohydrodynamic atomization. *Thin Solid Films* **520**, 6398–6403 (2012). doi:[10.1016/j.tsf.2012.06.050](https://doi.org/10.1016/j.tsf.2012.06.050)
40. M.N. Awais, N.M. Muhammad, D. Navaneethan, H.C. Kim, J. Jo, K.H. Choi, Fabrication of ZrO₂ layer through electrohydrodynamic atomization for the printed resistive switch (memristor). *Microelectron. Eng.* **103**, 167–172 (2013). doi:[10.1016/j.mee.2012.09.005](https://doi.org/10.1016/j.mee.2012.09.005)
41. M. Maria, D. Navaneethan, K.H. Chan, H.M. Taek, C.K. Hyun, Solution processed fabrication of single wall carbon nanotubes thin film by electrohydrodynamic atomization deposition technique and its characterization. *Appl. Phys. A* **109**, 515–522 (2012). doi:[10.1007/s00339-012-7302-y](https://doi.org/10.1007/s00339-012-7302-y)
42. K.H. Choi, A. Ali, J. Jo, Randomly oriented graphene flakes film fabrication from graphite dispersed in *N*-methyl-pyrrolidone by using electrohydrodynamic atomization technique. *J. Mater. Sci. Mater. Electron.* **24**, 4893–4900 (2013). doi:[10.1007/s10854-013-1494-6](https://doi.org/10.1007/s10854-013-1494-6)
43. N. Duraisamy, N.M. Muhammad, A. Ali, J. Jo, K.-H. Choi, Characterization of poly(3,4-ethylenedioxythiophene):poly(styrenesulfonate) thin film deposited through electrohydrodynamic atomization technique. *Mater. Lett.* **83**, 80–83 (2012). doi:[10.1016/j.matlet.2012.05.127](https://doi.org/10.1016/j.matlet.2012.05.127)
44. N. Duraisamy, N.M. Muhammad, M.T. Hyun, K.H. Choi, Structural and electrical properties of P3HT:PCBM/PEDOT:PSS thin films deposited through electrohydrodynamic atomization technique. *Mater. Lett.* **92**, 227–230 (2013). doi:[10.1016/j.matlet.2012.10.104](https://doi.org/10.1016/j.matlet.2012.10.104)
45. A.M. Gañán-Calvo, J. Dávila, A. Barrero, Current and droplet size in the electrospraying of liquids. Scaling laws. *J. Aerosol Sci.* **28**, 249–275 (1997). doi:[10.1016/S0021-8502\(96\)00433-8](https://doi.org/10.1016/S0021-8502(96)00433-8)
46. X. Zhang, J. Zhu, N. Haldolaarachchige, J. Ryu, D.P. Young, S. Wei et al., Synthetic process engineered polyaniline nanostructures with tunable morphology and physical properties. *Polymer* **53**, 2109–2120 (2012). doi:[10.1016/j.polymer.2012.02.042](https://doi.org/10.1016/j.polymer.2012.02.042)